Microchim Acta (2016) 183:329–336
DOI 10.1007/s00604-015-1630-5

ORIGINAL PAPER

A sol-gel based molecular imprint incorporating carbon dots for fluorometric determination of nicotinic acid

Pengli Zuo[1] · Junfa Gao[1] · Jun Peng[2] · Jianha Liu[1] · Mingming Zhao[1] · Jiahong Zhao[1] · Pengjian Zuo[4] · Hua He[2,3]

Received: 18 July 2015 / Accepted: 27 August 2015 / Published online: 30 September 2015
© Springer-Verlag Wien 2015

Abstract We are introducing functionalized carbon dots (C-dots) coated with a shell of molecularly imprinted sol-gel as a new tool in molecular imprint-based detection. Specifically, an imprint recognizing nicotinic acid (NA) was prepared in two steps. The first involves pyrolytic decomposition of citric acid in the presence of aminopropyltriethoxysilane to yield triethoxysilyl-modified C-dots with a typical size of 2.8 ± 1.1 nm. These are then polycondensed in the presence of tetraethoxysilane and NA at room temperature to give spherical silica nanoparticles (SiNPs) with a typical size of ~300 nm and containing C-dots and NA in the silica matrix. NA was then removed by extraction. The resulting SiNPs are well permeable to NA, photostable, display strong blue luminescence and can bind NA fairly selectively. The fluorometric detection scheme is based on the finding that increasing concentrations of NA quench the fluorescence of the C-dots in the SiNPs. NA can be determined by this method in the 0.5 to 10.5 μM concentration range, with a 12.6 nM detection limit. The composite was successfully utilized as a fluorescent probe for the determination of NA in spiked human urine samples. The method is believed to have a wider scope in being applicable to other analytes that are capable of quenching the fluorescence of C-dots.

Keywords Fluorescent probe · Surface modification · Silica particles · Quenching · Transmission electron microscopy · Pyrolysis

Electronic supplementary material The online version of this article (doi:10.1007/s00604-015-1630-5) contains supplementary material, which is available to authorized users.

✉ Hua He
dochehua@163.com; jcb315@163.com

[1] Central Laboratory, Yishui Central Hospital, Linyi 276400, China

[2] Department of Analytical Chemistry, China Pharmaceutical University, 24 Tongjia Lane, Nanjing, Jiangsu province 210009, China

[3] Key Laboratory of Drug Quality Control and Pharmacovigilance, Ministry of Education, China Pharmaceutical University, Nanjing 210009, China

[4] Laboratory of Chemistry, Yishui NO.4 High School, Linyi 276400, China

Introduction

Molecular imprinting technique refers to taking a particular target molecule as a template, and preparing a polymer which is specific for the molecule by simulating antigen-antibody interaction. Based on this theory, bulk molecularly imprinted polymers (MIPs) have been commonly prepared by self-assembly approach and applied for a wide scope [1], for instance, in separation processes, catalysis, antibody mimics and artificial enzymes. Because most binding sites are in the inner part of bulk MIPs, it is hard for the large molecules, especially proteins, to go into and out of the polymers [2]. The approach by using small molecule as template to prepare MIPs can effectively improve the adsorption capacity and specific identification of prepared polymers. A further improvement of their efficiency can be achieved by placing the active site inside soluble nanoparticles [3]. Many approaches have been developed for the preparation of MIPs. Among them, sol-gel process has many advantages, such as mild processing conditions, eco-friendly reaction solvent, etc. As we known, many kinds of MIPs with great sensitivity and selectivity necessary for sensing applications have been prepared by sol-gel approach [4].

C-dots are a class of nano-structured materials, which are strongly fluorescent, emission-color-tuning and non-blinking.

Owing to low cytotoxicity and impressive photostability of C-dots, they have garnered considerable interest since their discovery. Among the physicochemical characteristics of C-dots, their optical properties, especially their fluorescence emissions, have attracted considerable attention [5]. However, the main problem, lacking molecular recognition properties, has limited their application. With the increasing complexity and diversity of samples for drug analysis, the separation and detection of trace components have become a prominent issue.

As the increasing demand of complicated sample analysis, reports about the functional composite materials have increased greatly [6]. MIPs not only were synthesized on the surface of carbon nanotubes [7], but also have been combined with many other kinds of materials to prepare composite materials for a wider scope application. For instance, Lin et al. [8] synthesized MIPs thin films on the surface of CdSe/ZnS core-shell. Similarly, Lin et al. [9] used poly(ethylene-co-ethylene alcohol) as cross-linker to incorporate quantum dots into MIPs. Wang et al. [10] anchored the MIP layer on the surface of quantum dots via a surface molecular imprinting process using tetraethoxysilane as cross-linker. Some researchers have coated fluorescence C-dots with molecularly imprinted silica film by sol-gel polymerization approach [11]. Therefore, combining the molecular imprinting technique with fluorescence technique, functional composite materials can be prepared, which will not only have molecular specific identifying characteristics, but also show high optical sensitivity. These materials can be used as a fluorescent probe to detect trace substances in complex samples.

Nicotinic acid (NA) belongs to the vitamin B group. It participates in the oxidizing process of cells, lowers plasma levels of cholesterol, and maintains the normal functions of skin. NA has been widely used in medicine and food additives. Detection and quantification of NA are important in diagnoses and treatments of several disorders [12]. Different analytical methods have been developed for NA determination, including high-performance liquid chromatography (HPLC) [13], capillary electrophoresis [14], enzymic method [15] and supercritical fluid chromatography coupled to tandem mass spectrometry [16]. Enzymic method was not sensitive enough in some case. HPLC and capillary electrophoresis were susceptible to ambient temperature. Supercritical fluid chromatography coupled to tandem mass spectrometry has detection limit as low as 1 ng mL^{-1}, but this method is complex, expensive, and the sample has to be diluted with organic solvent. Therefore, low cost, sensitive and selective sensor systems have become increasingly needed for NA determinations.

To the best of our knowledge, there are no previous reports on NA fluorescent optosensing based on molecular imprinting technology. We describe the preparation of a fluorescent probe for NA detection. First of all, using anhydrous citric acid as precursor, we prepared silane groups coated C-dots [17]. Secondly, we used NA as template molecules, which were mixed with silane groups coated C-dots, functional monomer and cross-linker in ethanol, SiNPs were fabricated by sol-gel method. Once more, upon removal of the templates, the recognition specificity of SiNPs and the effect of NA on the fluorescence intensity were studied. Moreover, linear regression analysis was performed to assess the relationship between fluorescence response and NA concentration. Eventually, SiNPs were utilized as a fluorescent probe for the detection of NA in biological samples.

Experiment

Apparatus

Solution pH values were determined by use of a pHS-25 pH meter (Shanghai Albert Instrument Factory, China). UV–vis absorption was characterized by a UV1800 UV–vis spectrophotometer (Shimadzu Corporation, Japan). Photoluminescence emission measurements were performed using a RF-5301PC fluorescence spectrophotometer (Shimadzu Corporation, Japan). FT-IR spectrum was performed on a Shimadzu IR-prespige-21 FT-IR spectrometer (Kyoto, Japan) in the range of 400–4000 cm^{-1}. The morphology of the nanoparticles was studied using a JEM-2100 (HR) transmission electron microscope (TEM) (JEOL, Japan). The X-ray photoelectron spectra (XPS) of C-dots were obtained with an X-ray photoelectron spectrometer (K-Alpha, Thermo Fisher). Time-resolved fluorescence spectra were carried out in a time-correlated single-photon counting (TCSPC) system from an Edinburgh FLS920 spectrometer (Edinburgh Instruments, UK) excited at the wavelength of 370 nm. Dynamic light scattering studies and zeta potential measurements were recorded on a Malvern Instruments (Malvern, UK) Zetasizer Nano ZS90.

Materials and reagents

Ascorbic acid (AA) and isonicotinic acid (INA) were purchased from Sinopharm Chemical Reagent Co., Ltd. (Shanghai, China; www.reagent.com.cn), anhydrous citric acid was purchased from Shanghai Ziyi Reagent Factory (www.ziyi-reagent.com), 3-aminopropyl triethoxysilane (APTES), tetraethoxysilane (TEOS), ammonia solution (25 % in water) and NA were obtained from Aladdin (Shanghai, China; http://www.aladdin-e.com). Doubly deionized water was used throughout.

Fabrication of C-dots

The overall synthetic procedure is illustrated in Scheme. 1. C-dots were prepared from anhydrous citric acid according to the previously described method with some minor modifications

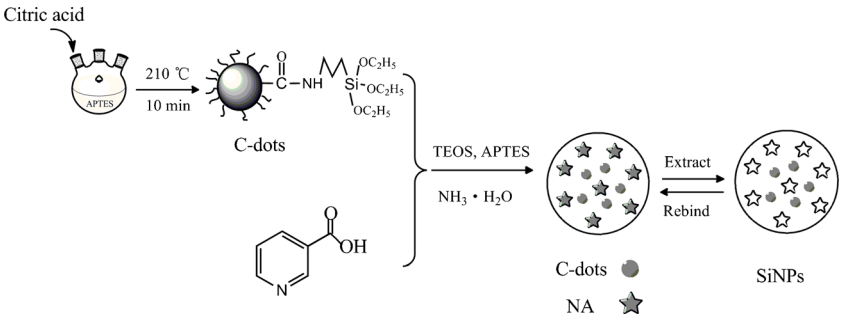

Scheme 1 Illustration of the preparation of silica nanoparticles (SiNPs)

[17]. 10 mL APTES was added into a 100 mL three-necked flask, purged with nitrogen, and was heated to 210 °C, then 0.5 g anhydrous citric acid was quickly added with vigorous stirring. After keeping the temperature at 210 °C for 10 min, the mixture was naturally cooled down to room temperature. The final product was separated by precipitation with petroleum ether, and was purified with dichloromethane to remove the unreacted organic moieties, then centrifuged at 10, 000 rpm. The obtained nanoparticles were dispersed in ethanol for the next process.

Synthesis of silica nanoparticles (SiNPs)

Nicotinic acid (NA; 30 mg) acting as the template was mixed with 18 mL of a solution of C-dots in ethanol (containing 1824 mg of C-dots) in a 50 mL flask, sonicated to dissolve NA. To the resulting mixture, 155 μL APTES (functional monomer) and 0.7 mL TEOS (cross-linker) were added under magnetic stirring. Finally, 430 μL water and 60 μL ammonia solution were added, the mixture was magnetically stirred for 24 h at room temperature.

After the reaction was finished, the solution became turbid, and a thick white emulsion was obtained. Then it was centrifuged at 3000 rpm, the white precipitate was washed with ethanol to discard the unreacted monomers. Templates in the composite were extracted with the mixture of methanol and acetic acid (9/1, *v*/*v*) several times, until the template molecules in the eluent were not detected with UV spectrometer at 263 nm. The obtained SiNPs were washed with water three times, dried at 60 °C in a vacuum drying oven overnight.

Following the same procedure, non-imprinted polymer nanoparticles were prepared as a control, except that no template was added.

Fluorescence properties of SiNPs

The obtained SiNPs were added into deionized water (pH 7.0), and 20 μg mL^{-1} mixed solution was prepared. 10 μL NA aqueous solution of certain concentration was diluted to produce 5 mL by adding the SiNPs solution, mixed thoroughly. After reaction for 8 min at room temperature, the fluorescence emission spectra were obtained by scanning the emission from 300 to 700 nm on the spectrofluorimeter. The measurement of non-imprinted polymer nanoparticles as control was the same as SiNPs.

Analytical application

Human urine samples were collected from healthy volunteers. 1 mL of urine sample was diluted with deionized water to 100 mL. 20 μg mL^{-1} SiNPs mixed solution was prepared using the diluted urine sample. 10 μL NA aqueous solution of certain concentration was diluted to produce 5 mL by adding the mixed solution, the resulting urine solutions were detected by the spectrofluorimeter. The amount of NA was determined according to the calibration curves.

Results and discussion

Selection of materials

Even though many composite materials have been prepared using quantum dots and organic cross-linkers, synthesis of conventional semiconductor quantum dots usually required laborious processes. Meanwhile, most of the metal-based quantum dots in use are toxic, resulting in environmental and biological hazards [5]. MIPs prepared using organic cross-linkers such as poly(ethylene-co-vinylalcohol) [9] were hydrophobic, so they are poorly water-soluble [18]. Furthermore, when quantum dots were wrapped in a shell of MIPs, their fluorescence intensity decreased and emission peak red-shifted, fluorescence property would change [8]. To solve the above-mentioned questions, C-dots have inspired extensive studies. C-dots have unique attributes, such as benign chemical composition, high aqueous solubility, low toxicity, good biocompatibility, facile functionalization, non-photobleaching, low cost and easy of synthesis [19]. What's more, C-dots with high quantum yields have been fabricated by hydrothermal method [20]. Silica matrix is a kind of inert and transparent material [21], composite materials using TEOS as cross-linker can keep the photoluminescence properties of C-dots. Because of many hydrophilic hydroxyl groups on the surface of SiNPs, they are water-soluble and

their imprinting efficiency can be improved. So C-dots and organic silanes are applicable as initial materials to synthesize SiNPs.

Characterization of C-dots

Highly luminescent C-dots functionalized with triethoxysilane groups were prepared via a pyrolytic process. The functionalized C-dots were characterized with FTIR spectroscopy, TEM and fluorescent spectroscopy.

The TEM image (Fig. 1a) showed that the C-dots with microspherical shape were uniform, mono-dispersed. A particle diameter of 2.8 ± 1.1 nm was estimated from TEM image by investigating 87 particles, which was consistent with the dynamic light scattering result (Fig. S1, Electronic Supplementary Material, ESM). The zeta potential of the C-dots in water at pH 7.0 was measured to be 3.51 mV. In the process of C-dots synthesis, anhydrous citric acid was decomposited and carbonized under high temperature conditions. Surface passivation was achieved using the reaction of the amine group in APTES with the carboxyl groups on the surface of pyrolyzed organics, thereby achieving bright luminescence and surface functionalization of C-dots simultaneously [17].

FT-IR spectra comparison between APTES and C-dots was shown in Fig. 2a. Spectra of APTES and C-dots displayed some common characteristic absorption bands. The FTIR peak at 3456 cm^{-1} was ascribed to N-H stretching vibration. The peak at 1078 cm^{-1} corresponded to O-Si-O asymmetric stretching vibration. The peak at 1554 cm^{-1} was attributed to secondary amine R-NH-R bending vibration, 1639 cm^{-1} was attributed to the stretching vibration of secondary amide carbonyl (C = O). The two typical signals of C-dots (1554, 1639 cm^{-1}) demonstrated that acylation reaction had occurred between C-dots and APTES, and that silane groups had been connected on the surface of C-dots via amido linkage. The surface elemental analysis for the resultant nanoparticles was determined by XPS. The full range XPS analysis (Fig. 2b) of the resultant C-dots clearly showed four peaks at 284.08, 399.08, 531.08 and 101.58 eV, which were attributed to C 1 s, N 1 s, O 1 s and Si 2p, respectively. Functionalization of C-dots was further confirmed by the XPS result.

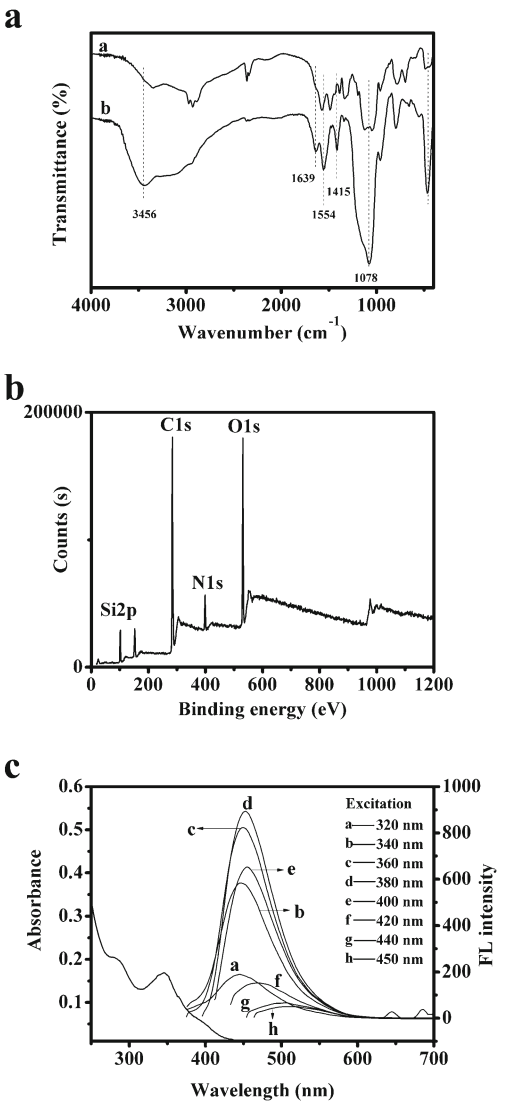

Fig. 2 FT-IR spectra of APTES (**a**) and C-dots (**b**) **a**. Survey XPS spectra of C-dots **b**. UV–vis absorption spectra and photoluminescence spectra of C-dots excited at the wavelength from 320 to 450 nm **c**

The fluorescent emission spectra were detected by scanning the emission from 300 to 700 nm on the spectrofluorimeter (with 5 and 5 nm slit width for excitation and emission, respectively). Figure 2c depicted the UV–vis absorption and photoluminescence spectra of C-dots in ethanol. The maximum UV absorption peak was observed at 360 nm. When

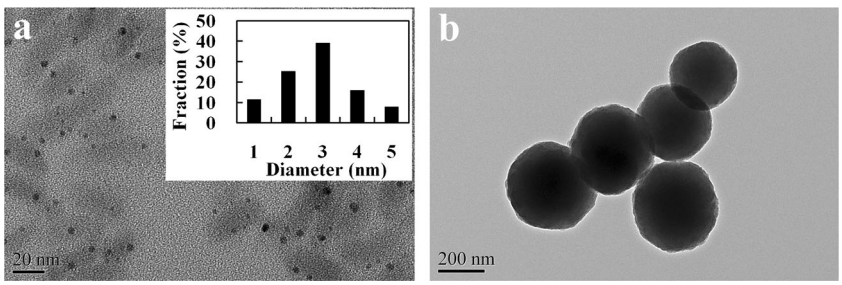

Fig. 1 **a** TEM images of C-dots; scale bars: 20 nm. **b** TEM images of SiNPs; scale bars: 200 nm

excited at the wavelength from 320 to 450 nm, the C-dots showed blue-green photoluminescence. The fluorescent intensity gradually increased with increasing excitation wavelength from 320 to 380 nm, the photoluminescence spectra showed the highest fluorescence intensity when C-dots were excited at 380 nm, however, the fluorescent intensity gradually decreased as the excitation wavelength continued increasing. The emission peak position shifted from 448 nm to 507 nm with increasing excitation wavelength from 320 to 450 nm. Their emission spectra were highly dependent on the excitation wavelength.

Characterization of SiNPs

Catalyzed by aqueous ammonia, polymerization took place on the surface of C-dots through the hydrolysis and condensation reaction of APTES and TEOS, MIPs were successfully anchored on the surface of C-dots. The morphology of the SiNPs was characterized by TEM. As shown in Fig. 1b, the resulting particles showed spherical nanostructure with ca. 300 nm diameter, and they were in relatively narrow size distribution.

The fluorescent emission spectra of SiNPs in ethanol were detected by scanning the emission from 350 to 700 nm on the spectrofluorimeter. As shown in Fig. 3, with the decrease of the incident light wavelength, the ultraviolet absorption of SiNPs (unlabelled curve) gradually increased, but no UV absorption peak was observed. When excited from 320 nm to 360 nm, the fluorescence intensity of SiNPs gradually increased, the maximum fluorescence emission peak at 452 nm was obtained when excited at 360 nm. From 360 nm to 390 nm, with the excitation wavelength increasing, the fluorescence intensity gradually decreased. These results demonstrated that the silica coating had little influence on the fluorescence intensity of C-dots [22]. Different from C-dots, the emission peak position of SiNPs had no shift as the excitation wavelength increasing from 320 to 390 nm. This phenomenon might be caused by fluorescence resonance energy transfer [23]. The C-dots acted as donors, MIPs served as acceptors, this donor-acceptor system lead to intra-energy transfer [24], so there were no wavelength shifts.

The fluorescence intensity of an aqueous solution of SiNPs (20 μg mL^{-1}) was recorded every 5 min under 360 nm excitation. As shown in Fig. S2 (ESM), the fluorescence intensity of SiNPs in water was relatively strong and stable.

Recognition capability of SiNPs

Figure 4 compared the FTIR spectra between non-imprinted polymer nanoparticles and SiNPs. All spectra exhibited strong N-H stretching vibration at 3438 cm^{-1}. The presence of the carbonyl group in the spectrum of SiNPs before template molecules extraction was confirmed by the peak at 1668 cm^{-1}, corresponding to the C = O stretching mode. The characteristic peak at 1486 cm^{-1} was attributed to pyridine ring skeletal vibration of NA molecule. The presence of pyridine ring and carbonyl group peaks in the spectrum of SiNPs before template molecules extraction, combined with the absence of these characteristic peaks after solvent elution, demonstrated the successful imprinting of NA into the silica matrix. The broad and strong peak around 1078 cm^{-1} was assigned to the O-Si-O asymmetric stretching vibration, and the peaks at 458 cm^{-1} and 795 cm^{-1} were assigned to the Si-O stretching vibration. The peak at 1638 cm^{-1} was attributed to the stretching vibration of secondary amide carbonyl (C = O). All these bonds demonstrate that molecular imprint incorporating C-dots have successfully been prepared by sol-gel condensation approach.

As shown in Fig. 5a, b and c, after template extraction, the fluorescence intensity of SiNPs increased greatly, while quenched a lot when interacted with NA solution. These spectra confirmed that the extraction and rebinding of NA were a reversible process.

The selectivity adsorption of the SiNPs was investigated with INA and AA as the reference compound. As can be seen from Fig. 5b, the fluorescence responses of SiNPs towards

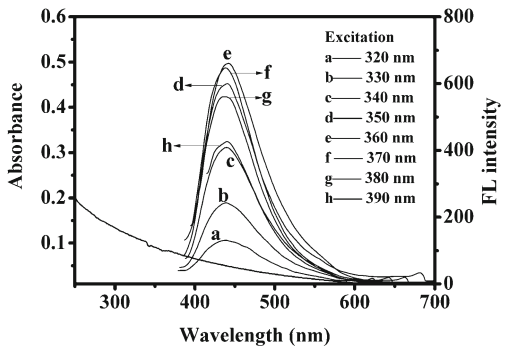

Fig. 3 UV–vis absorption spectrum and Photoluminescence spectra of SiNPs excited at the wavelength from 320 to 390 nm

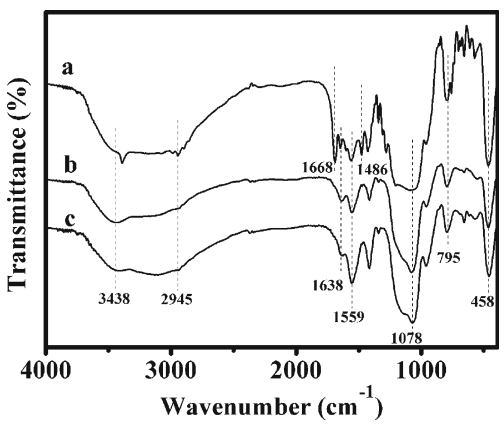

Fig. 4 FT-IR spectra of non-imprinted polymer nanoparticles (**c**), SiNPs before (**a**) and after (**b**) template molecules extraction

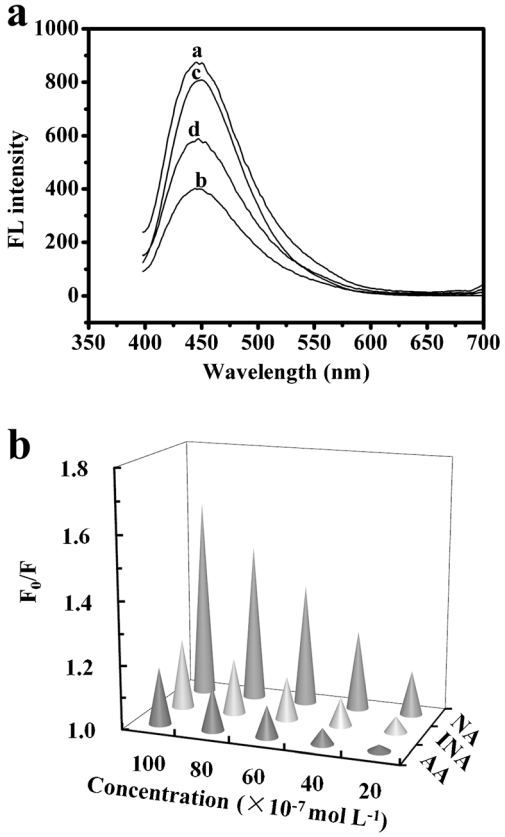

Fig. 5 Fluorescence emission spectra of non-imprinted polymer nanoparticles (**a**), SiNPs before (**b**) and after (**c**) template extraction, SiNPs (20 μg mL^{-1}) with addition of aqueous solution of NA (**d**) **a**. Selectivity adsorption of SiNPs **b**

NA were much larger than its structure analogues AA and INA, which indicated SiNPs had better adsorption and binding capacity for the template molecules. With increasing concentration of NA, fluorescence quenching degree increased. Because of nonspecific adsorption, there were some fluorescence responses towards AA and INA, but much lower than that of NA. After the removal of template molecules, imprinted cavities and specific binding sites in a predetermined orientation were formed. The shapes of the cavities were fit for the unique molecular structure of NA, but the imprinted cavities were not suitable for other structure analogues. Other analogues were not bound tightly in the imprinted cavities. This was attributed to the imprinting effect, different molecular interactions and their specific structures [25], so the SiNPs had highly specific recognition for the template molecules.

Template measurement

The fluorescence intensity of the SiNPs at 452 nm (exCitation 360 nm) gradually decreased with increment of NA concentration, revealing that this method was sensitive to NA concentration in aqueous solution. The photoluminescence quenching data followed the Stern-Volmer equation:

$$^{F_0}/_{F} = 1 + K_{SV}[C_{NA}]$$

F and F_0 are the fluorescent intensities of the SiNPs in the presence and absence of NA respectively. [C_{NA}] is the concentration of NA, K_{SV} is the quenching constant of the quencher (NA). The fluorescence quenching efficiency of SiNPs was 2.8 times as large as that of non-imprinted polymer nanoparticles, which confirmed the efficient imprinting effect of SiNPs. Owing to better steric matching of recognition sites with NA in the SiNPs, more template molecules were adsorbed in the imprinted silica matrix via hydrogen bonds and van der Wall forces [26], leading to C-dots fluorescence quenching. To get further insight into the fluorescence quenching mechanism, the time-resolved fluorescence of SiNPs in the presence and absence of NA was performed under the excitation of 370 nm (Fig. S3, ESM). After adding NA solution, the decay time of SiNPs changed little, indicating that a static mechanism dominated for the quenching [27, 28]. Calibration for NA was constructed from the fluorescence spectra results with concentration increment of NA, and a linear regression equation was obtained as follows:

$$^{F_0}/_{F} = 1 + 5.85 \times 10^4[C_{NA}]$$

A good linear relationship was observed up to NA concentration ranging from 0.5 to 10.5 μM with a correlation coefficient of 0.9981. K_{SV} was found to be 5.85×10^4 L mol^{-1}. The detection limit, calculated according to the 3σ IUPAC criteria, was 12.6 nM.

Applications of SiNPs

Urine of healthy adults was diluted 100-fold with deionized water, 20 μg mL^{-1} SiNPs mixed solution was prepared using the diluted urine. Determinations were carried out for a set of measurements of 10, 50 and 100×10^{-7} M of NA in diluted urine, respectively. Table 1 showed that the quantification results of NA were in good agreement with the added values. The recovery was calculated as the ratio of the responses of NA obtained from the spiked urine against those of the standard solutions at the same levels (n = 6, average of six

Table 1 Determination of urine sample by this method (n = 6)

Urine sample	Added NA ($\times 10^{-7}$ M)	Average founded ($\times 10^{-7}$ M)	Recovery (%)	RSD (%)
1	10.00	9.76	97.60	4.76
2	50.00	49.64	99.28	4.21
3	100.00	101.12	101.12	3.45

Table 2 Figures of merits of nanomaterial-based methods for determination of NA

Methods	Linear range	LOD	Comments	Reference
MIP-Voltammetric determination	0.05–5 mM		High selectivity, quick detection; Low correlation coefficient; Determination in aqueous solution	[29]
Micellar liquid chromatography	0.05–50 μg mL^{-1}	8 ng mL^{-1}	Selective; Time-consuming, using organic solvent	[30]
Micellar electrokinetic chromatography	10–100 μM	0.3 μg mL^{-1}	Good linearity, accuracy and precision; Depending on surfactant concentration and pH; Determination in aqueous solution	[31]
Ion chromatograph	0.5–10 mg L^{-1}	0.2 mg L^{-1}	High selectivity, robust; Low recovery, using organic solvents	[32]
RP-HPLC	0.05–500 mg L^{-1}	0.25 mg kg^{-1}	Wide linear range, good precision; Using organic solvents	[33]
LC-MS/MS	2.0–3000 ng mL^{-1}	–	Specific and sensitive; High cost; Using organic solvents	[34]
Biochemical assay	1–1000 μM	–	High-throughput measurement; Time consuming, complicated, non-linear, high cost; Determination in aqueous solution	[35]
Fluorescent probe	0.5–10.5 μM	12.6 nM	Easy synthesis and low cost, sensitive, high selectivity; Determination in aqueous solution	This work

replicate measurements), and the RSD were 4.76 %, 4.21 % and 3.45 %, respectively. These values indicated that this method was accurate and precise.

Table 2 summarized the detection limit, linear range and comments using different methods for the determination of NA. Our method was comparable with micellar liquid chromatography [30], micellar electrokinetic chromatography with ultraviolet detector [31] and reverse phase high-performance liquid chromatography [33]. The results demonstrate that this method offers a facile and selective approach for the detection of NA in urine solution.

Conclusions

A facile method for the highly selective recognition of NA was developed based on the combination of the fluorescence and molecularly imprinting techniques. C-dots were prepared at relatively low temperature in APTES. Using NA as template molecules, SiNPs were fabricated by sol-gel polymerization at room temperature. The fabrication process was facile without any complex or post-treatment procedures. The starting materials are low cost and easily available. The fabricated SiNPs showed some advantages such as strong fluorescence, stability and monodispersity. They were used as optical sensor, which selectively bound to the template molecules. A good linear relationship between fluorescence intensity ratio of the system and concentration of NA in aqueous solution was observed in a wide response range. Furthermore, the method was successfully developed for the determination of trace NA in human urine samples. Combining their low cost, stability, selectivity and convenient synthesis, we expect the method will play an important role in probing other analytes which can quench the fluorescence of C-dots.

Acknowledgments This work was supported by Graduate Students Innovative Projects of Jiangsu Province (No.CXZZ12_0308). We thank the editors and co-workers for help and constructive suggestions.

References

1. Vlatakis G, Andersson LI, Muller R, Mosbach K (1993) Drug assay using antibody mimics made by molecular imprinting. Nature 361: 645–647. doi:10.1038/361645a0
2. Ge Y, Turner AP (2008) Too large to fit? Recent developments in macromolecular imprinting. Trends Biotechnol 26(4):218–224. doi:10.1016/j.tibtech.2008.01.001
3. Wulff G (2013) Fourty years of molecular imprinting in synthetic polymers: origin, features and perspectives. Microchim Acta 180(15–16):1359–1370. doi:10.1007/s00604-013-0992-9
4. Gupta R, Kumar A (2008) Molecular imprinting in sol-gel matrix. Biotechnol Adv 26(6):533–547. doi:10.1016/j.biotechadv.2008.07.002
5. Lim SY, Shen W, Gao ZQ (2015) Carbon quantum dots and their applications. Chem Soc Rev 44:362–381. doi:10.1039/C4CS00269E
6. Shughart EL, Ahsan K, Detty MR, Bright FV (2006) Site selectively templated and tagged xerogels for chemical sensors. Anal Chem 78(9):3165–3170. doi:10.1021/ac060113m
7. Dai H, Xiao DL, He H, Li H, Yuan DH, Zhang C (2015) Synthesis and analytical applications of molecularly imprinted polymers on the surface of carbon nanotubes: a review. Microchim Acta. doi:10.1007/s00604-014-1376-5
8. Lin CI, Joseph AK, Chang CK, Lee YD (2004) Synthesis and photoluminescence study of molecularly imprinted polymers

appended onto CdSe/ZnS core-shells. Biosens Bioelectron 20(1): 127–131. doi:10.1016/j.bios.2003.10.017
9. Lin HY, Ho MS, Lee MH (2009) Instant formation of molecularly imprinted poly(ethylene-co-vinyl alcohol)/quantum dot composite nanoparticles and their use in one-pot urinalysis. Biosens Bioelectron 25(3):579–586. doi:10.1016/j.bios.2009.03.039
10. Wang HF, He Y, Ji TR, Yan XP (2009) Surface molecular imprinting on Mn-doped ZnS quantum dots for room-temperature phosphorescence optosensing of pentachlorophenol in water. Anal Chem 81(4):1615–1621. doi:10.1021/ac802375a
11. Mao Y, Bao Y, Han DX, Li FH, Niu L (2012) Efficient one-pot synthesis of molecularly imprinted silica nanospheres embedded carbon dots for fluorescent dopamine optosensing. Biosens Bioelectron 38(1):55–60. doi:10.1016/j.bios.2012.04.043
12. Carlson LA (2005) Nicotinic acid: the broad-spectrum lipid drug. A 50th anniversary review. J Intern Med 258(2):94–114. doi:10.1111/j.1365-2796.2005.01528.x
13. Pfuhl P, Karcher U, Haring N, Baumeister A, Tawab MA, Schubert-Zsilavecz M (2005) Simultaneous determination of niacin, niacinamide and nicotinuric acid in human plasma. J Pharm Biomed Anal 36(5):1045–1052. doi:10.1016/j.jpba.2004.08.033
14. Iwaki M, Murakami E, Kikuchi M, Wada A, Ogiso T, Oda Y, Kubo K, Kakehi K (1998) Simultaneous determination of nicotinic acid and its metabolites in rat urine by micellar electrokinetic chromatography with photodiode array detection. J Chromatogr B Biomed Sci Appl 716(1–2):335–342. doi:10.1016/S0378-4347(98)00327-2
15. HamanoT MY, Kojima N, Aoki N, Semma M, Ito Y, Oji Y (1995) Enzymic method for the amperometric determination of nicotinic acid in meat products. Analyst 120:135–138. doi:10.1039/AN9952000135
16. Taquchi K, Fukusaki E, Bamba T (2014) Determination of niacin and its metabolites using supercritical fluid chromatography coupled to tandem mass spectrometry. Mass Spectrom (Tokyo) 3(1):A0029. doi:10.5702/massspectrometry.A0029
17. Wang F, Xie Z, Zhang H, Liu CY, Zhang YG (2011) Highly luminescent organosilane-functionalized carbon dots. Adv Funct Mater 21(6):1027–1031. doi:10.1002/adfm.201002279
18. Chen L, Xu S, Li J (2011) Recent advances in molecular imprinting technology: current status, challenges and highlighted applications. Chem Soc Rev 40:2922–2942. doi:10.1039/C0CS00084A
19. Ding CQ, Zhu AW, Tian Y (2014) Functional surface engineering of C-dots for fluorescent biosensing and in vivo bioimaging. Acc Chem Res 47(1):20–30. doi:10.1021/ar400023s
20. Zhu SJ, Meng QN, Wang L, Zhang JH, Song YB, Jin H, Zhang K, Sun HC, Wang HY, Yang B (2013) Highly photoluminescent carbon dots for multicolor patterning, sensors, and bioimaging. Angew Chem 125(14):4045–4049. doi:10.1002/ange.201300519
21. Yang Y, Gao MY (2005) Preparation of fluorescent SiO_2 particles with single CdTe nanocrystal cores by the reverse microemulsion method. Adv Mater 17(19):2354–2357. doi:10.1002/adma.200500403
22. Sun J, Zhuang JQ, Guan SW, Yang WS (2008) Synthesis of robust water-soluble ZnS:Mn/SiO_2 core/shell nanoparticles. J Nanoparticle Res 10(4):653–658. doi:10.1007/s11051-007-9296-5
23. Dong YQ, Wang RX, Li GL, Chen CQ, Chi YW, Chen GN (2012) Polyamine-functionalized carbon quantum dots as fluorescent probes for selective and sensitive detection of copper ions. Anal Chem 84(14):6220–6224. doi:10.1021/ac3012126
24. Lunz M, Bradley AL, Chen WY, Gerard VA, Byrne SJ, Gun'ko YK, Lesnyak V, Gaponik N (2010) Influence of quantum dot concentration on förster resonant energy transfer in monodispersed nanocrystal quantum dot monolayers. Phys Rev B 81:201356. doi:10.1103/PhysRevB.81.205316
25. Wang X, Fang Q, Liu S, Chen L (2012) Preparation of a magnetic molecularly imprinted polymer with pseudo template for rapid simultaneous determination of cyromazine and melamine in biomatrix samples. Anal Bioanal Chem 404(5):1555–1564. doi:10.1007/s00216-012-6200-7
26. Li HB, Li YL, Cheng J (2010) Molecularly imprinted silica nanospheres embedded CdSe quantum dots for highly selective and sensitive optosensing of pyrethroids. Chem Mater 22(8):2451–2457. doi:10.1021/cm902856y
27. Lakowicz J (2006) Principles of fluorescence spectroscopy. Springer Science Business Media, New York
28. Backhus DA, Golini C, Castellanos E (2003) Evaluation of fluorescence quenching for assessing the importance of interactions between nonpolar organic pollutants and dissolved organic matter. Environ Sci Technol 37(20):4717–4723. doi:10.1021/es026388a
29. Yao LD, Tang YW, Huang ZF (2007) Nicotinic acid voltammetric sensor based on molecularly imprinted polymer membrane-modified electrode. Anal Lett 40(4):677–688. doi:10.1080/00032710601017755
30. Capella-Peiró ME, Carda-Broch S, Monferrer-Pons L, Esteve-Romero J (2004) Micellar liquid chromatographic determination of nicotinic acid and nicotinamide after precolumn könig reaction derivatization. Anal Chim Acta 517(1–2):81–87. doi:10.1016/j.aca.2004.05.014
31. Zhang J, Chakraborty U, Foley JP (2009) Determination of residual cell culture media components by MEKC. Electrophoresis 30(22): 3971–3977. doi:10.1002/elps.200900169
32. Saccani G, Tanzi E, Mallozzi S, Cavalli S (2005) Determination of niacin in fresh and dry cured pork products by ion chromatography: experimental design approach for the optimisation of nicotinic acid separation. Food Chem 92(2):373–379. doi:10.1016/j.foodchem.2004.10.007
33. Ciulu M, Solinas S, Floris I, Panzanelli A, Pilo MI, Piu PC, Spano N, Sanna G (2011) RP-HPLC determination of water-soluble vitamins in honey. Talanta 83(3):924–929. doi:10.1016/j.talanta.2010.10.059
34. Liu M, Zhang D, Wang XL, Zhang LN, Han J, Yang M, Xiao X, Zhang YN, Liu HC (2012) Simultaneous quantification of niacin and its three main metabolites in human plasma by LC–MS/MS. J Chromatogr B 904:107–114. doi:10.1016/j.jchromb.2012.07.030
35. Graeff R, Lee HC (2002) A novel cycling assay for nicotinic acid–adenine dinucleotide phosphate with nanomolar sensitivity. Biochem J 367:163–168. doi:10.1042/BJ20020644